PERGAMON

Automatica 36 (2000) 1153–1169

www.elsevier.com/locate/automatica

Control of underactuated spacecraft with bounded inputs[☆]

Panagiotis Tsiotras[a,]*, Jihao Luo[b]

[a]*School of Aerospace Engineering, Georgia Institute of Technology, Atlanta, GA 30332-0150, USA*
[b]*Department of Mechanical and Aerospace Engineering, University of Virginia, Charlottesville, VA 22903-2442, USA*

Received 1 December 1998; revised 18 October 1999; received in final form 18 December 1999

Bounded feedback control laws are designed for stabilization and tracking of underactuated spacecraft. The flat outputs of the system are computed and are used to generate reference trajectories for the tracking problem.

Abstract

We provide stabilizing feedback control laws for the kinematic system of an underactuated axisymmetric spacecraft subject to input constraints. The proposed control law forces all closed-loop trajectories in a region of the state space where the control inputs are small and bounded. The control law is subsequently extended to solve the case of attitude tracking for an underactuated spacecraft using two controls. As a special case we also provide a feedback control for the spacecraft symmetry axis to track a specified direction in the inertial space. All proposed control laws achieve asymptotic stability with exponential convergence. In addition, we give a methodology for generating feasible trajectories using the fact that the system is differentially flat. One of the novelties of the proposed control design is the use of a non-standard description of the attitude motion, which allows the decomposition of the general motion into two rotations. This attitude description is especially useful for analyzing axisymmetric bodies, where the motion of the symmetry axis is of prime importance. © 2000 Elsevier Science Ltd. All rights reserved.

Keywords: Attitude control; Satellite control; Saturation; Tracking; Asymptotic stability; Differential flatness

1. Introduction

The problem of attitude stabilization has been the subject of numerous research articles in the last decade (Crouch, 1984; Byrnes & Isidori, 1991; Wen & Kreutz-Delgado, 1991; Krishnan, McClamroch & Reyhanoglu, 1992; Bach & Paielli, 1993; Tsiotras, Corless & Longuski, 1995). Most of these results deal with the case of complete control actuation. A complete mathematical description of the attitude stabilization problem was presented as early as 1984 by Crouch (1984), where he provided the necessary and sufficient conditions for the controllability of a rigid body in the case of one, two and three independent control torques. This sparked a renewed interest in the area of control of rigid spacecraft with less than three control torques. Stabilization of the angular velocity equations was addressed, for example, by Aeyels and Szafranski (1988), Sontag and Sussmann (1988), Outbib and Sallet (1992) and Andriano (1993). The complete set of attitude equations (including the kinematics) was addressed in Byrnes and Isidori (1991) where they established that a rigid spacecraft controlled by two pairs of gas-jet actuators cannot be asymptotically stabilized to an equilibrium using a smooth feedback control law. Subsequently, in Krishnan et al. (1992) and later in Tsiotras et al. (1995), nonsmooth controllers were established to stabilize an axisymmetric spacecraft. Since the complete dynamics of the spacecraft fail to be controllable or even accessible (Krishnan et al., 1992), both of these controllers achieve arbitrary reorientation of the spacecraft, only for the restricted case of zero spin rate. This is an interesting control problem because, similarly to the nonsymmetric case (Byrnes & Isidori, 1991), any stabilizing (time-invariant) control law has to be necessarily nonsmooth. Time-varying stabilizing control laws have been reported in Coron and Kerai (1996), Morin and Samson

[☆]The original version of this paper was presented at the IFAC Symposium Nonlinear Control Systems (NOLCOS) which was held in Enschede, The Netherlands during July, 1998. This paper was recommended for publication in revised form by Associate Editor H. Khalil under the direction of Editor T. Basar.

* Corresponding author. Tel.: + 1-(404)-894-9526; fax: + 1-(404)-894-2760.

E-mail address: p.tsiotras@ae.gatech.edu (P. Tsiotras).

PII: S0005-1098(00)00025-X

(1997) and Morin, Samson, Pomet and Jiang (1995). In addition, as was shown in Sørdalen, Egeland and Canudas de Wit (1992), the underactuated axi-symmetric rigid body reorientation problem is equivalent to a three-wheel mobile robot or, equivalently, to the well-studied nonholonomic integrator benchmark problem in the area of nonholonomic systems. Khennouf and Canudas de Wit (1995) have shown how to construct discontinuous controllers for a nonholonomic system in power form, by extending the results of Tsiotras et al. (1995). The controllers in Tsiotras et al. (1995) and Khennouf and Canudas de Wit (1995), in particular, are not Lipschitz continuous at the equilibrium, and may require significant amounts of control effort, especially if the initial conditions are close to an equilibrium manifold. In Tsiotras and Luo (1997) this controller was modified, to remedy the problem of large control inputs. The procedure in Tsiotras and Luo (1997) consists of dividing the state space into two regions. The control law drives the trajectories of the closed-loop system away from the singular equilibrium manifold (which gives rise to high control inputs) and into the region in the state space where the high authority part of the control input remains small. No a priori bounds on the control input where given in Tsiotras and Luo (1997), however.

In this paper, we continue the approach initiated in Tsiotras and Luo (1997) and derive a controller for the kinematics of an axisymmetric spacecraft with two inputs (and zero spin rate) which remains bounded by an a priori specified bound. We make use of the formulation for the attitude kinematics developed in Tsiotras and Longuski (1995) and Tsiotras and Longuski (1996). This attitude description allows one to isolate and describe the motion of the symmetry axis of the body using a single complex variable. We also solve the problem of tracking an attitude trajectory for an axisymmetric spacecraft with two control inputs. The tracking problem is formulated as one of tracking a "virtual" spacecraft which follows the target trajectory. The control law is exponentially convergent and remains bounded by a specified upper bound. As a special case, we present a feedback control law so that the spacecraft symmetry axis tracks a specified direction in inertial space. In the final section of the paper we address the problem of on-line feasible trajectory generation for an underactuated body with two controls. We use the notion of *differential flatness* (Fliess, Levine, Martin & Rouchon, 1992, 1995) and we propose a simple way for designing the trajectory in the flat output space. Several numerical examples demonstrate the theoretical developments of the paper.

The main contribution of the paper stems from the development of bounded ("saturating") control laws for both the stabilization and the tracking problems of an underactuated axi-symmetric body subject to two controls. No similar results have been reported in the literature, at least as far as the authors know. We also propose a specific approach for generating feasible reference state trajectories for the tracking problem. Although the property of differential flatness for the underactuated rigid body problem has been known for some time (Nieuwstadt & Murray, 1995) no actual results have appeared in the literature dealing specifically with this problem.

The discussion in the paper is confined to the kinematic level, i.e., it is assumed that one can issue directly angular velocity commands. The implementation of the angular velocity commands via the dynamics is not pursued here. How accurately these commands can be followed depends on the bandwidth of the spacecraft actuators (e.g., thrusters, reaction/momentum wheels, control moment gyros, etc.). For "fast-enough" actuators, a singular perturbation approach similar to the one in Tsiotras and Luo (1997), can be used to implement the angular velocity commands. Although we cannot guarantee *explicit* bounds on the actual torques, the results of Tsiotras and Luo (1997) show that highly oscillatory angular velocity commands (which will be typically responsible for the high torques) are avoided by keeping the trajectories away from the singular equilibrium manifold.

Finally, it should be pointed out that because of the connection to nonholonomic systems, the methodology proposed in this paper can be used for stabilization and tracking of general nonholonomic systems in either power of chained form. Some initial results in this direction have appeared in Luo and Tsiotras (1998).

2. The (w, z) attitude parameterization

The orientation of a rigid spacecraft can be specified using various parameterizations, for example, Eulerian Angles, Euler Parameters, Cayley–Rodrigues Parameters, etc.; see, for instance, the recent survey article by Shuster (1993). Recently, a new parameterization using a pair of a complex and a real coordinate was introduced based on an extension of an old result by Darboux (Darboux, 1887; Tsiotras & Longuski, 1995, 1996). According to the results of Tsiotras et al. (1995) the relative orientation between two reference frames can be represented by *two successive rotations*. The first rotation is about the inertial $\hat{\imath}_3$-axis at an angle z. The second rotation is about the unit vector

$$\hat{h} = \left(\frac{w + \bar{w}}{2|w|}\right)\hat{\imath}'_1 + \left(\frac{\mathrm{i}(\bar{w} - w)}{2|w|}\right)\hat{\imath}'_2 \tag{1}$$

and has magnitude

$$\theta = \arccos\left(\frac{1 - |w|^2}{1 + |w|^2}\right). \tag{2}$$

In Eq. (1), $\hat{\mathbf{i}}' = (\hat{\imath}'_1, \hat{\imath}'_2, \hat{\imath}'_3)$ is the intermediate reference frame resulting from the rotation z about the inertial

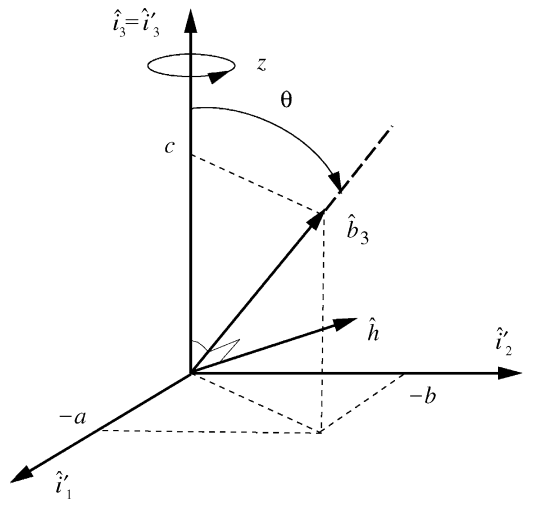

Fig. 1. Attitude description in terms of (w, z) coordinates.

$\hat{\imath}_3$-axis. The situation is depicted in Fig. 1, where (a, b, c) denote the coordinates of the unit vector $\hat{\imath}'_3$ in the body frame, $\hat{\imath}'_3 = a\hat{b}_1 + b\hat{b}_2 + c\hat{b}_3$. It can be shown (Tsiotras & Longuski, 1995) that the location of the body $\hat{b}_3$-axis in the $\hat{\mathbf{i}}'$ frame is also determined by a, b, c from $\hat{b}_3 = -a\hat{\imath}'_1 - b\hat{\imath}'_2 + c\hat{\imath}'_3$ (Fig. 1). With this notation, the complex coordinate w is defined by

$$w = w_1 + \mathrm{i}w_2 = \frac{b - \mathrm{i}a}{1 + c}. \tag{3}$$

We note here that in Eqs. (1) and (3), $\mathrm{i} = \sqrt{-1}$, bar denotes the complex conjugate, and $|w|^2 = w\bar{w}$ denotes the absolute value of the complex number $w \in \mathbb{C}$. Conversely, from w one can compute (a, b, c) from

$$a = \mathrm{i}\frac{w - \bar{w}}{1 + |w|^2}, \quad b = \frac{w + \bar{w}}{1 + |w|^2}, \quad c = \frac{1 - |w|^2}{1 + |w|^2}. \tag{4}$$

The rotation matrices corresponding to the two rotations in the (w, z) kinematic description have been calculated in Tsiotras and Longuski (1995) as

$$R_1(z) = \begin{bmatrix} \cos z & \sin z & 0 \\ -\sin z & \cos z & 0 \\ 0 & 0 & 1 \end{bmatrix},$$

$$R_2(w) = \frac{1}{1 + |w|^2}\begin{bmatrix} 1 + \mathrm{Re}(w^2) & \mathrm{Im}(w^2) & -2\,\mathrm{Im}(w) \\ \mathrm{Im}(w^2) & 1 - \mathrm{Re}(w^2) & 2\,\mathrm{Re}(w) \\ 2\,\mathrm{Im}(w) & -2\,\mathrm{Re}(w) & 1 - |w|^2 \end{bmatrix}, \tag{5}$$

where $\mathrm{Re}(\cdot)$ and $\mathrm{Im}(\cdot)$ denote the real and imaginary parts of a complex number. Subsequently, the rotation matrix from the inertial to body frame is given by

$$R(w, z) = R_2(w)R_1(z) \tag{6}$$

which can be written in the form

$$R(w, z) = \frac{1}{1 + |w|^2}$$

$$\begin{bmatrix} \mathrm{Re}[(1 + w^2)\mathrm{e}^{\mathrm{i}z}] & \mathrm{Im}[(1 + w^2)\mathrm{e}^{\mathrm{i}z}] & -2\,\mathrm{Im}(w) \\ \mathrm{Im}[(1 - \bar{w}^2)\mathrm{e}^{-\mathrm{i}z}] & \mathrm{Re}[(1 - \bar{w}^2)\mathrm{e}^{-\mathrm{i}z}] & 2\,\mathrm{Re}(w) \\ 2\,\mathrm{Im}(w\mathrm{e}^{\mathrm{i}z}) & -2\,\mathrm{Re}(w\mathrm{e}^{\mathrm{i}z}) & 1 - |w|^2 \end{bmatrix}. \tag{7}$$

Conversely, given a proper rotation matrix R, one can compute w and z and decompose the motion in two rotations. The following lemma states this result.

Lemma 1. *For any rotation matrix* R, *let*

$$w = \frac{R_{23} - \mathrm{i}R_{13}}{1 + R_{33}} \tag{8}$$

and

$$\cos z = \tfrac{1}{2}((1 + |w|^2)\mathrm{trace}(R) + |w|^2 - 1) \tag{9a}$$

$$\begin{aligned} \sin z &= \frac{1}{1 + |w|^2}[(1 + \mathrm{Re}(w^2))R_{12} \\ &\quad + \mathrm{Im}(w^2)R_{22} + 2\,\mathrm{Im}(w)R_{32}] \\ &= -\frac{1}{1 + |w|^2}[\mathrm{Im}(w^2)R_{11} \\ &\quad + (1 - \mathrm{Re}(w^2))R_{21} - 2\,\mathrm{Re}(w)R_{31}] \end{aligned} \tag{9b}$$

with the matrices $R_1(z)$ *and* $R_2(w)$ *as in Eqs.* (5). *Then* $R(w, z) = R_1(w)R_2(z)$ *with* w *and* z *as in Eqs.* (8) *and* (9).

The proof is straightforward and thus, omitted.

From now on, and by virtue of Lemma 1, we can refer to (w, z) as the "attitude coordinates" for the matrix R without any ambiguity.

The kinematic equations in terms of w and z can be written as follows (Tsiotras et al., 1995; Tsiotras & Longuski, 1995):

$$\dot{w} = -\mathrm{i}\omega_3 w + \frac{\omega}{2} + \frac{\bar{\omega}}{2}w^2, \tag{10a}$$

$$\dot{z} = \omega_3 + \mathrm{Im}(\omega\bar{w}), \tag{10b}$$

where $\omega = \omega_1 + \mathrm{i}\omega_2$.

In this paper we assume that only the angular velocity ω (equivalently, ω_1 and ω_2) can be manipulated. The angular velocity component about the body $\hat{b}_3$-axis, ω_3, cannot be changed due to, say, a thruster failure. Specifically, for an axisymmetric body about the body $\hat{b}_3$-axis with no torque component about this axis, ω_3 remains constant for all $t \geq 0$. In this case, three-axis stabilization and pointing is possible only if, in addition, $\omega_3 \equiv 0$.[1] This

[1] Of course, stabilization and inertial pointing of the symmetry axis is still possible; see, for example, Krishnan et al. (1992) and Tsiotras and Longuski (1994).

case will arise, for instance, during a rest-to-rest maneuver of an axisymmetric spacecraft.

Letting $\omega_3 = 0$ the kinematic equations become

$$\dot{w} = \frac{\omega}{2} + \frac{\bar{\omega}}{2}w^2, \tag{11a}$$

$$\dot{z} = \mathrm{Im}(\omega\bar{w}). \tag{11b}$$

In Tsiotras et al. (1995) the following feedback control law was proposed in order to stabilize the system in Eq. (11):

$$\omega = -\kappa w - \mathrm{i}\mu\frac{z}{\bar{w}}, \quad \mu > \kappa/2. \tag{12}$$

This control law is well defined for $w(0) \neq 0$, but initial conditions close to the manifold $w = 0$ may result to high control inputs. The next section proposes a control law which avoids this problem by ensuring that the control input ω remains below a specified upper bound.

3. Stabilization with bounded control

Without any further modification, the domain of validity of the system in Eqs. (12) is the set of pairs $(w,z)\in(\mathbb{C}\backslash\{0\})\times S^1$. For $w(0) = 0$ the control law can be modified by using any open-loop strategy of arbitrary short duration (Tsiotras et al., 1995). Nevertheless, Eq. (12) suggests that the control inputs may become arbitrarily large for initial conditions close to the manifold $w = 0$ (and $z \neq 0$). In addition, Eq. (12) suggests that the control input ω will remain "small" if the trajectories belong to, say, the set

$$\mathscr{D}_\mathrm{g} = \{(w,z)\in\mathbb{C}\times S^1\colon |z|/|w| \leq 1\}. \tag{13}$$

We seek to construct a control law that will keep all trajectories in $\mathscr{D}_\mathrm{g}$ and force the trajectories outside $\mathscr{D}_\mathrm{g}$ to enter this set in finite time.

Before we state the main result in this section, we need the following definition.

Definition 2. Given two scalars $z\in\mathbb{R}$ and $w\in\mathbb{C}$, we define the *complex saturating function* $\mathrm{sat_c}(\cdot)$ by

$$\mathrm{sat_c}(z,w) = \begin{cases} 0 & \text{if } z = 0, w = 0, \\ \mathrm{sat}\left(\dfrac{z}{|w|}\right)\mathrm{e}^{\mathrm{i}\phi} & \text{if } w \neq 0, \\ \mathrm{sgn}(z) & \text{if } z \neq 0, w = 0 \end{cases} \tag{14}$$

and $\phi = \arg(w)$ is the argument of w, i.e., $w = |w|\mathrm{e}^{\mathrm{i}\phi}$.

The function $\mathrm{sat_c}(\cdot)$ is defined for all $(w,z)\in\mathscr{D} := \mathbb{C}\times S^1$. Fig. 2 shows this function for *real* and positive w. Note that $\mathrm{sat_c}(\cdot)$ is discontinuous at the origin.

The following proposition provides a stabilizing control law which is bounded by a specified constant.

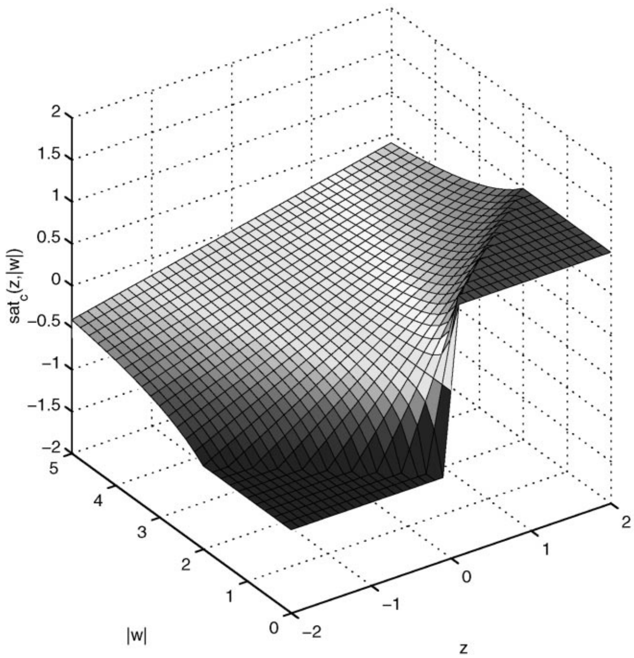

Fig. 2. A depiction of the function $\mathrm{sat_c}(z,w)$ for real and positive w.

Proposition 3. *Consider the system in Eq.* (11) *and the following control law*:

$$\omega = -\kappa\frac{w}{\sqrt{1+|w|^2}} - \mathrm{i}\mu\,\mathrm{sat_c}(z,w), \tag{15}$$

where $\mathrm{sat_c}(z,w)$ *is as in Definition* 2, *and where* κ *and* μ *are constants satisfying*

$$\mu > \kappa/2 > 0 \quad \textit{if } (w,z)\in\mathscr{D}_\mathrm{g}, \tag{16a}$$

$$\mu > -\kappa > 0 \quad \textit{if } (w,z)\in\mathscr{D}_\mathrm{b} := \mathscr{D}\backslash\mathscr{D}_\mathrm{g}. \tag{16b}$$

Then, for all initial conditions $(w(0),z(0))\in\mathscr{D}$, *the control law in Eq.* (15) *is well defined and the corresponding closed-loop trajectories satisfy* $\lim_{t\to\infty}(w(t),z(t)) = 0$. *In addition, the control law is bounded as* $|\omega(t)| \leq \max\{|\kappa|\} + \mu$ *for all* $t \geq 0$, *where* $\max\{|\kappa|\}$ *denotes the maximum of the absolute value of* κ *in* $\mathscr{D}_\mathrm{b}$ *and* $\mathscr{D}_\mathrm{g}$.

Consider the positive-definite, radially unbounded function $V\colon \mathbb{C}\times\mathbb{R}\to\mathbb{R}_+$ defined by $V(w,z) = 2(\sqrt{1+|w|^2} - 1) + \frac{1}{2}z^2$. Noticing that

$$\frac{\mathrm{d}}{\mathrm{d}t}|w|^2 = (1+|w|^2)\,\mathrm{Re}(\omega\bar{w}), \tag{17}$$

the derivative of V along the closed-loop trajectories yields

$$\begin{aligned} \dot{V} &= \frac{1}{\sqrt{1+|w|^2}}(1+|w|^2)\,\mathrm{Re}(\omega\bar{w}) + z\,\mathrm{Im}(\omega\bar{w}) \\ &= -\sqrt{1+|w|^2}\frac{\kappa|w|^2}{\sqrt{1+|w|^2}} - \mu z\,\mathrm{Im}[\mathrm{sat_c}(z,w)\,\bar{w}] \\ &= -\kappa|w|^2 - \mu z\,\mathrm{sat}\left(\frac{z}{|w|}\right)|w|. \end{aligned} \tag{18}$$

If $(w,z) \in \mathscr{D}_b$ then $|z|/|w| > 1$ and $z\,\mathrm{sat}(z/|w|) = z\,\mathrm{sgn}(z) = |z|$. Since $\mu > -\kappa > 0$ one obtains from Eq. (18)

$$\dot{V} = -|w|^2(\kappa + \mu|z|/|w|) < -|w|^2(\kappa + \mu) < 0 \tag{19}$$

for all $(w,z) \in \mathscr{D}_b$. Notice also that in $\mathscr{D}_b$, $V \geq 2(\sqrt{1+|w|^2} - 1) + \frac{1}{2}|w|^2$. The last equation, along with Eq. (19) imply that if the trajectories remain in $\mathscr{D}_b$, then $\lim_{t\to\infty} |w(t)| = 0$. This leads to a contradiction, since

$$\frac{\mathrm{d}}{\mathrm{d}t}|w|^2 = -\kappa|w|^2\sqrt{1+|w|^2} \tag{20}$$

with $\kappa < 0$, and $|w|$ is monotonically increasing in $\mathscr{D}_b$. Therefore, the trajectories leave $\mathscr{D}_b$ and enter the region $\mathscr{D}_g$ in finite time. Moreover, for $(w,z) \in \mathscr{D}_g$ we have that $|z|/|w| \leq 1$ and hence from Eq. (18)

$$\dot{V} = -\kappa|w|^2 - \mu z^2 < 0 \quad \forall (w,z) \in \mathscr{D}_g \tag{21}$$

since $\kappa > 0$ for $(w,z) \in \mathscr{D}_g$.

We have shown that $\dot{V} < 0$ for all $(w,z) \in \mathscr{D}$ and hence $\lim_{t\to\infty} V(t) = 0$. In particular, $\lim_{t\to} (w(t), z(t)) = 0$. The asymptotic convergence to the origin is exponential, as can be easily seen by checking the closed-loop system for $(w,z) \in \mathscr{D}_g$,

$$\frac{\mathrm{d}}{\mathrm{d}t}|w|^2 = -\kappa|w|^2\sqrt{1+|w|^2} \leq -\kappa|w|^2, \tag{22a}$$

$$\frac{\mathrm{d}z}{\mathrm{d}t} = -\mu z. \tag{22b}$$

Moreover, a straightforward calculation shows that

$$|\omega(t)| \leq |\kappa|\frac{|w(t)|}{\sqrt{1+|w(t)|^2}} + \mu \leq \max\{|\kappa|\} + \mu \tag{23}$$

for all $t \geq 0$ and the control law is bounded.

The motivation behind the proposed control law is simple. It forces all trajectories to the "good" region $\mathscr{D}_g$ where the potentially bothersome term $z/\bar{w}$ in Eq. (12) is bounded by a known constant. Moreover, Eqs. (22) show that if $\mu > \kappa/2$ the vector fields on $|z| = |w|$ point in the interior of $\mathscr{D}_g$ and thus, $\mathscr{D}_g$ is a positively invariant set of the closed-loop trajectories. Once in $\mathscr{D}_g$, Eqs. (22) ensure that trajectories go to the origin with exponential rate of decay. As a result, there is at most one switching as the control law crosses the boundary $|z| = |w|$ and there is no possibility of chattering. Although the control law in Eq. (15) is discontinuous, the solutions of the closed-loop system are well defined and unique.

Remark 4. The idea of dividing the state space into "good" and "bad" regions was initially used in Tsiotras and Luo (1997). Nevertheless, the control law in Tsiotras and Luo (1997) guarantees only convergence to the origin. Here, by virtue of inequalities (19) and (21) we are actually able to prove asymptotic (Lyapunov) *stability* for the closed-loop system.[2] In addition, in Tsiotras and Luo (1997) no a priori upper bound of the control law was given.

Remark 5. We can use Eq. (22) to introduce a sliding mode defined by the equation $|z| = |w|$ by making the vector field on the boundary of $\mathscr{D}_g$ point to the interior of $\mathscr{D}_b$. This can be achieved by choosing, for example, $\kappa > 2\mu$ in Eq. (16a). Then for $|z| = |w|$, we get $\mathrm{sat}_c(z,w) = \mathrm{sgn}(z)\mathrm{e}^{\mathrm{i}\phi}$ and the equations become

$$\frac{\mathrm{d}}{\mathrm{d}t}|w|^2 = -\kappa(1+|w|^2)|w|^2, \tag{24a}$$

$$\frac{\mathrm{d}z}{\mathrm{d}t} = -\mu\,\mathrm{sgn}(z)|z|. \tag{24b}$$

The previous equations show that the sliding mode is stable.

Fig. 3(a) shows the sets $\mathscr{D}_b$ and $\mathscr{D}_g$ in the $(|w|, |z|)$ space, along with typical trajectories for the closed-loop system in Eq. (11) with the control law in Eq. (15). Fig. 3(b) shows the corresponding trajectories when choosing $\kappa > 2\mu$ in $\mathscr{D}_g$. The trajectories tend to the origin along the sliding mode described by the boundary of the sets $\mathscr{D}_g$ and $\mathscr{D}_b$, i.e., along $|z| = |w|$ (see also Remark 5 above).

Recall that the previous derivation assumes that $\omega_3 \equiv 0$. In practice, there is always a small coupling between the axes due to system imperfections. For a spacecraft with small asymmetries the equation for ω_3 is given by $\dot{\omega}_3 = \varepsilon\omega_1\omega_2$ where ε is a constant parameter that depends on the body moments of inertia. In this case the body will spin about the z-axis. The best one can hope for in this case is a very slow rotation about this axis. Numerical simulations indicate that this drift is typically small for small asymmetries ($\varepsilon \ll 1$) and $\omega_3(0) = 0$. If $\omega_3(0) \neq 0$, the procedure described in Schleicher (1999) can be used to first drive ω_3 (and w) to zero using ω as the control input. After this preliminary step a control law such as in Eq. (12) or Eq. (15) can be applied.

4. Tracking of an underactuated spacecraft

In this section we derive a controller for an underactuated spacecraft to track a desired attitude. The desired attitude history is given in terms of the complex/real attitude parameters of Section 2 as $w_d(t)$ and $z_d(t)$. These parameters represent the orientation of a "virtual" spacecraft in *inertial* space. Because $\omega_3 \equiv 0$, the attitude parameters of the spacecraft w and z cannot be functionally

[2] Asymptotic stability is here defined with respect to the subspace topology of $\mathbb{C} \times S^1$ generated by the open subset $(\mathbb{C}\backslash\{0\}) \times S^1$.

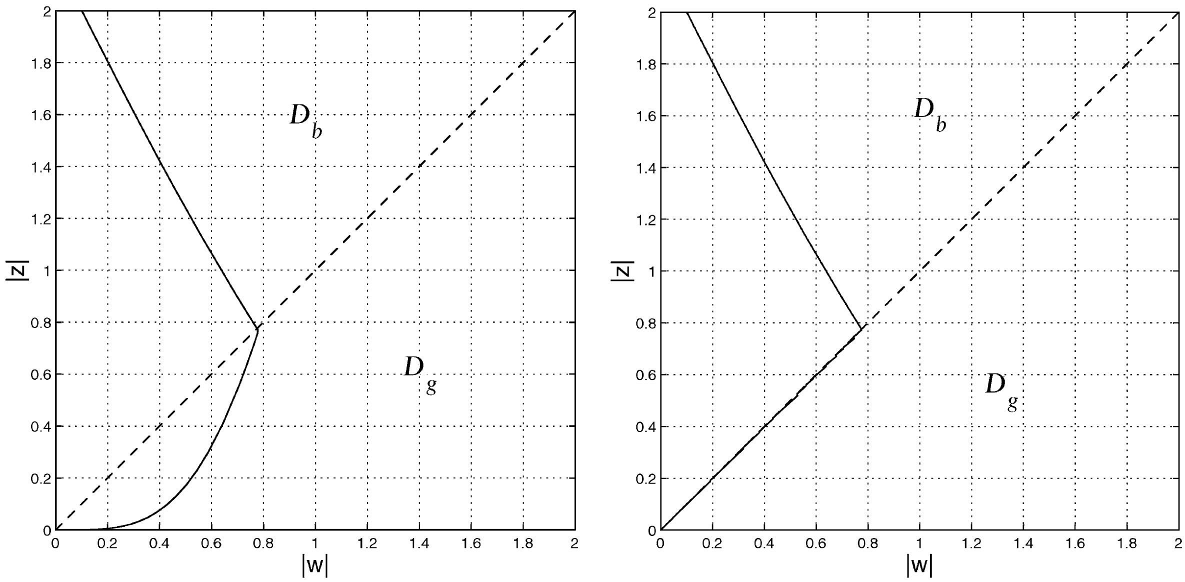

(a) Closed-loop trajectories with control in Eq. (15).

(b) Sliding mode for the case $\kappa > 2\mu$ in $\mathscr{D}_g$.

Fig. 3. Typical closed-loop trajectories for the system of equations (11)–(15) and the sets $\mathscr{D}_b$ and $\mathscr{D}_g$.

independent. In other words, in the absence of any control over ω_3, we cannot expect to track arbitrary trajectories. In order for the underactuated spacecraft to properly track the target attitude, it is reasonable to assume that the target attitude trajectory, $w_d(t), z_d(t)$, is generated by two control angular velocities $\omega_{d_1}(t), \omega_{d_2}(t)$ of a "virtual" spacecraft. This will guarantee that the corresponding trajectories are *feasible*. In Section 6 we will remove this restriction and we will develop an approach to generate feasible trajectories between two given attitude orientations. Feasibility of trajectories ensures that there exist $\omega_{d1}(t)$ and $\omega_{d2}(t)$ such that Eqs. (25) are satisfied for all $t \geq 0$.

The governing kinematic equations for this "virtual" spacecraft are of the same form as in Eqs. (11)

$$\dot{w}_d = \frac{\omega_d}{2} + \frac{\bar{\omega}_d}{2} w_d^2, \tag{25a}$$

$$\dot{z}_d = \mathrm{Im}(\omega_d \bar{w}_d), \tag{25b}$$

where $\omega_d = \omega_{d_1} + \mathrm{i}\omega_{d_2}$ is the complex variable of the known angular velocities expressed in the "virtual" frame. They are assumed to be bounded by $|\omega_{d_i}(t)| \leq \beta_i$ for $i = 1,2$.

We wish to design a control law $\omega = \omega(w, z, \omega_d, w_d, z_d)$ such that it satisfies the following two requirements:

Tracking control requirements:

(R1) If $w(0) = w_d(0)$ and $z(0) = z_d(0)$ then $w(t) = w_d(t)$ and $z(t) = z_d(t)$ for all $t \geq 0$ (perfect tracking).

(R2) For all initial conditions $(w(0), z(0)) \in \mathbb{C} \times S^1$ we have that $\lim_{t\to\infty} (w(t), z(t)) = (w_d(t), z_d(t))$ (asymptotic tracking).

To make things more concrete, let the inertial frame be $\hat{\mathbf{i}} = (\hat{\imath}_1, \hat{\imath}_2, \hat{\imath}_3)$, the body frame of the spacecraft be $\hat{\mathbf{b}} = (\hat{b}_1, \hat{b}_2, \hat{b}_3)$, and the reference frame of the "virtual" spacecraft be $\hat{\mathbf{v}} = (\hat{v}_1, \hat{v}_2, \hat{v}_3)$. It is easy to see that

$$\hat{\mathbf{b}} = R(w, z)\hat{\mathbf{i}} \quad \text{and} \quad \hat{\mathbf{v}} = R(w_d, z_d)\hat{\mathbf{i}}. \tag{26}$$

We can then express the body frame of the spacecraft in the reference frame of the "virtual" spacecraft as follows: $\hat{\mathbf{b}} = R(w, z)R^{\mathrm{T}}(w_d, z_d)\hat{\mathbf{v}} := R_r(w_r, z_r)\hat{\mathbf{v}}$ where $R_r(w_r, z_r)$ is the rotation matrix from $\hat{\mathbf{v}}$ to $\hat{\mathbf{b}}$ and where w_r and z_r are the corresponding attitude coordinates. Lemma 1 shows how to compute (w_r, z_r) from (w, z) and (w_d, z_d), which can then serve as a coordinate description of the relative orientation between the $\hat{\mathbf{b}}$ and $\hat{\mathbf{v}}$ frames.

The angular velocity between the frames $\hat{\mathbf{b}}$ and $\hat{\mathbf{v}}$ (expressed in the $\hat{\mathbf{b}}$ frame) is given by

$$\begin{bmatrix} \omega_{r_1} \\ \omega_{r_2} \\ \omega_{r_3} \end{bmatrix} = \begin{bmatrix} \omega_1 \\ \omega_2 \\ 0 \end{bmatrix} - R_r(w_r, z_r) \begin{bmatrix} \omega_{d_1} \\ \omega_{d_2} \\ 0 \end{bmatrix}. \tag{27}$$

Note, in particular, that since $R_{r_{31}}$ and $R_{r_{32}}$ are nonzero, in general, $\omega_{r_3} \neq 0$, although both ω_3 and ω_{d_3} are assumed to be zero.

The kinematic equations of the target frame (as seen from $\hat{\mathbf{b}}$) are therefore given by

$$\dot{w}_r = -\mathrm{i}\omega_{r_3} w_r + \frac{\omega_r}{2} + \frac{\bar{\omega}_r}{2} w_r^2, \tag{28a}$$

$$\dot{z}_r = \omega_{r_3} + \mathrm{Im}(\omega_r \bar{w}_r). \tag{28b}$$

The objective of the tracking controller is to keep the body frame of the spacecraft aligned with the body frame of the target frame. Hence, the problem of tracking has been transformed to a problem of stabilization of the relative attitude expressed by the pair (w_r, z_r).

Proposition 6. *Let the kinematics of the spacecraft described by Eqs.* (11), *and the kinematics of the target attitude trajectory generated by Eqs.* (25) *for some known* $\omega_d(t)$. *Consider the controller*

$$\omega = -\kappa w_r - \mathrm{i}\left(\frac{\mu z_r + \omega_{r_3}}{\bar{w}_r}\right) + \eta(R_r, \omega_d), \tag{29}$$

where w_r *and* z_r *the attitude coordinates corresponding to the rotation matrix* R_r *from the target to the body frame,* $\kappa > 0$ *and* $\mu > \kappa/2$ *are constants, and*

$$\omega_{r3} = -R_{r_{31}}\omega_{d_1} - R_{r_{32}}\omega_{d_2}, \tag{30a}$$

$$\eta(R_r, \omega_d) = R_{r_{11}}\omega_{d_1} + R_{r_{12}}\omega_{d_2} + \mathrm{i}(R_{r_{21}}\omega_{d_1} + R_{r_{22}}\omega_{d_2}). \tag{30b}$$

Then this kinematic controller is well defined for all $t \geq 0$, *and for all initial conditions such that* $w(0) \neq w_d(0)$, *we have that* $\lim_{t\to\infty}(w(t), z(t)) = (w_d(t), z_d(t))$. *In addition, this controller is bounded along closed-loop trajectories.*

First, notice that with ω as in Eq. (29) the relative angular velocity between $\hat{\mathbf{b}}$ and $\hat{\mathbf{v}}$ is given by

$$\omega_r := \omega_{r_1} + \mathrm{i}\omega_{r_2} = -\kappa w_r - \mathrm{i}\left(\frac{\mu z_r + \omega_{r_3}}{\bar{w}_r}\right). \tag{31}$$

Substituting the previous equation in Eqs. (28) one obtains

$$\frac{\mathrm{d}}{\mathrm{d}t}|w_r|^2 = -\kappa |w_r|^2(1 + |w_r|^2), \tag{32a}$$

$$\frac{\mathrm{d}z_r}{\mathrm{d}t} = -\mu z_r \tag{32b}$$

and thus, $\lim_{t\to\infty}(w_r(t), z_r(t)) = 0$ with exponential rate of decay for all $(w_r, z_r) \in \mathscr{D}$.

The control law in Eq. (31) is well defined for all initial conditions $(w_r, z_r) \in (\mathbb{C}\backslash\{0\}) \times S^1$ since if $w_r(0) \neq 0$, Eq. (32a) implies that $w_r(t) \neq 0$ for all $t \geq 0$.

It remains to show that the control law in Eq. (31) is bounded. From Eq. (32a) one readily obtains that w_r is bounded. Moreover, using Eqs. (32) a direct calculation shows that $z_r/\bar{w}_r$ is bounded if $\mu > \kappa/2$. In addition, from Eq. (30a) one obtains that

$$\begin{aligned}\frac{|\omega_{r_3}|}{|w_r|} &\leq \frac{|R_{r_{31}}|}{|w_r|}|\omega_{d_1}| + \frac{|R_{r_{32}}|}{|w_r|}|\omega_{d_2}| \\ &\leq \frac{2}{1 + |w_r|^2}(|\omega_{d_1}| + |\omega_{d_2}|) \leq 2(\beta_1 + \beta_2),\end{aligned} \tag{33}$$

where we have used Eq. (7) and the facts that $|\mathrm{Re}(we^{\mathrm{i}z})| \leq |w|$ and $|\mathrm{Im}(we^{\mathrm{i}z})| \leq |w|$ for any $w \in \mathbb{C}$. Also, since R_r is a rotation matrix, a direct calculation shows that

$$|\eta(R_r, \omega_d)| \leq |\omega_d| \leq |\omega_{d_1}| + |\omega_{d_2}| = \beta_1 + \beta_2 \tag{34}$$

and $\eta(R_r, \omega_d)$ is bounded. Thus, ω is bounded. This completes the proof of the proposition.

A tracking controller bounded by a *given* upper bound can be obtained by simply combining the results of Propositions 3 and 6. Here we assume that this upper bound is greater than a constant that depends on the bounds of ω_{d_1} and ω_{d_2}. This is a reasonable assumption since there will always be a minimum effort required to track arbitrary trajectories. Moreover, this minimum effort will depend on the trajectories to be tracked.

Theorem 7. *Let the kinematics of a spacecraft described by Eqs.* (11), *and the kinematics of a target attitude trajectory generated by Eqs.* (25) *where* $|\omega_{d_i}(t)| \leq \beta_i$, *for* $i = 1,2$. *Consider a constant* $\beta_3 > 3(\beta_1 + \beta_2)$. *Let the feedback control law*

$$\begin{aligned}\omega = &-\kappa \frac{w_r}{\sqrt{1 + |w_r|^2}} - \mathrm{i}\mu\, \mathrm{sat_c}(z_r, w_r) \\ &- \mathrm{i}\frac{\omega_{r_3}}{\bar{w}_r} + \eta(R_r, \omega_d),\end{aligned} \tag{35}$$

where $w_r, z_r, R_r, \omega_{r_3}$, *and* $\eta(R_r, \omega_d)$ *as in Proposition* 6. *Assume that the gains* κ *and* μ *are as in Eq.* (16) *and that satisfy* $\max\{|\kappa|\} + \mu \leq \beta_3 - 3(\beta_1 + \beta_2)$. *Then the control law in Eq.* (35) *is well defined for all* $(w, z) \in \mathscr{D}$, *satisfies requirements* (R1) *and* (R2) *and it is bounded by* $|\omega(t)| \leq \beta_3$ *for all* $t \geq 0$.

Notice that if $w_r = 0$ then necessarily $\omega_{r_3} = 0$. Also, in this case, $\eta(R_r, \omega_d) = \omega_d\, \mathrm{e}^{-\mathrm{i}z_r}$. Thus, the control law in Eq. (35) simplifies to

$$\omega = -\kappa \frac{w_r}{\sqrt{1 + |w_r|^2}} - \mathrm{i}\mu\, \mathrm{sat_c}(z_r, w_r) + \omega_d\, \mathrm{e}^{-\mathrm{i}z_r}. \tag{36}$$

With the proposed control law in Eq. (35), the closed-loop trajectories satisfy

$$\frac{\mathrm{d}}{\mathrm{d}t}|w_r|^2 = -\kappa |w_r|^2\sqrt{1 + |w_r|^2}, \tag{37a}$$

$$\frac{\mathrm{d}z_r}{\mathrm{d}t} = -\mu\, \mathrm{sat}\left(\frac{z_r}{|w_r|}\right)|w_r|. \tag{37b}$$

By Proposition 3 it follows that $\lim_{t\to\infty}(w_r(t), z_r(t)) = 0$ for all $(w_r, z_r) \in \mathscr{D}$. If initially $w(0) = w_d(0)$ and $z(0) = z_d(0)$ then $R_r = I$ and the control law in Eq. (35) reduces to $\omega = \omega_d$ and thus, $(w(t), z(t)) = (w_d(t), z_d(t))$ for all $t \geq 0$. Therefore, the proposed control law satisfies requirements (R1) and (R2).

The proof of boundedness of ω is shown easily by

$$|\omega| \leq \max\{|\kappa|\} + \mu + \frac{|\omega_{r_3}|}{|w_r|} + |\eta(R_r,\omega_d)|$$

$$\leq \max\{|\kappa|\} + \mu + 3(\beta_1 + \beta_2) \leq \beta_3 \tag{38}$$

for all $t \geq 0$ where we have used Eqs. (33) and (34).

5. Special case: tracking of the symmetry axis

The results of the previous section can also be used in the special case of tracking a specific *direction* in inertial space with the body $\hat{b}_3$-axis (which we assume to be the symmetry axis of the axisymmetric spacecraft). This would be the case when, for example, the symmetry axis is the axis of a communications antenna, the line-of-sight of an onboard telescope or camera, etc. In all these cases, the relative rotation about the symmetry axis is irrelevant. In particular, the body is now allowed to rotate about its $\hat{b}_3$-axis at a constant angular rate $\omega_3(0) = \omega_{30}$.

It is assumed that the desired pointing direction with respect to the inertial frame is given as $w_d(t)$. Consulting Fig. 1, this implies that the desired direction in inertial frame is given by the unit vector

$$\hat{v}_3 = -a_d\hat{\imath}_1 - b_d\hat{\imath}_2 + c_d\hat{\imath}_3, \tag{39}$$

where

$$w_d = \frac{b_d - \mathrm{i}a_d}{1 + c_d}. \tag{40}$$

Conversely, given w_d, the coordinates of the vector $\hat{v}_3$ in the inertial frame $(-a_d, -b_d, c_d)$ can be computed from Eqs. (4). A tracking controller's objective is then to make $\hat{b}_3$ track $\hat{v}_3$ as $t \to \infty$.

Proposition 8. *Consider the system of Eqs.* (10) *describing the orientation of a rigid spacecraft in inertial frame. Let the direction along the unit vector in inertial frame given by* $\hat{v}_3$ *as described by Eqs.* (25a), (39) *and* (40), *where* $\omega_d(t) = \omega_{d_1} + \mathrm{i}\omega_{d_2}(t)$ *is a given function of time such that* $|\omega_{d_i}(t)| \leq \beta_i$ *for* $i = 1,2$. *Let the control law*

$$\omega = -\kappa\frac{w_r}{\sqrt{1 + |w_r|^2}} + \eta(R,\omega_d), \tag{41}$$

where $\kappa > 0$, *and where*

$$\eta(R,\omega_d) = R_{11}\omega_{d_1} + R_{12}\omega_{d_2} + \mathrm{i}(R_{21}\omega_{d_1} + R_{22}\omega_{d_2}) \tag{42}$$

with $R = R(w,z)$ *as in Eq.* (7). *Then with this control law the body* $\hat{b}_3$*-axis will track exponentially the direction along the unit vector* $\hat{v}_3$ *from all initial conditions. Moreover, the control law is bounded by* $|\omega(t)| \leq \kappa + \beta_1 + \beta_2$ *for all* $t \geq 0$.

Using the fact that $\hat{v}_3 = -a_d\hat{\imath}_1 - b_d\hat{\imath}_2 + c_d\hat{\imath}_3$ and $\hat{\mathbf{b}} = R(w,z)\hat{\mathbf{\imath}}$ one can immediately show that the target direction $\hat{v}_3$ in the body frame is given by

$$\hat{v}_3 = a_r\hat{b}_1 + b_r\hat{b}_2 + c_r\hat{b}_3, \tag{43}$$

where

$$\begin{bmatrix} a_r \\ b_r \\ c_r \end{bmatrix} = R(w,z)\begin{bmatrix} -a_d \\ -b_d \\ c_d \end{bmatrix}. \tag{44}$$

Using this expression, one can compute the "error" coordinate w_r in the body frame by

$$w_r = \frac{b_r - \mathrm{i}a_r}{1 + c_r}. \tag{45}$$

The differential equation for w_r is then given by Eq. (28a), where

$$\begin{bmatrix} \omega_{r_1} \\ \omega_{r_2} \\ \omega_{r_3} \end{bmatrix} = \begin{bmatrix} \omega_1 \\ \omega_2 \\ \omega_{30} \end{bmatrix} - R(w,z)\begin{bmatrix} \omega_{d_1} \\ \omega_{d_2} \\ 0 \end{bmatrix}. \tag{46}$$

Using the control law in Eq. (41), the closed-loop system for w_r yields

$$\frac{\mathrm{d}}{\mathrm{d}t}|w_r|^2 = -\kappa|w_r|^2(1 + |w_r|^2) \tag{47}$$

which shows that $w_r \to 0$ with exponential convergence rate. Eq. (43) shows that $w_r = 0$ implies that $a_r = b_r = 0$ and hence $\hat{v}_3 = \hat{b}_3$. Finally, using Eq. (34) it follows immediately that the control law is bounded by $|\omega(t)| \leq \kappa + \beta_1 + \beta_2$ for all $t \geq 0$.

Remark 9. The complex variable w_r denotes the "error" between the $\hat{v}_3$ and $\hat{b}_3$ unit vectors. However, notice that $w_r = 0$ does not necessarily imply that $w = w_d$. This is due to our specific definitions for w and w_d.

6. Feasible trajectory generation

In the tracking problem of Section 4 we assumed that the reference trajectory is given as the output of a dynamical system with the same nonlinear structure as the original system. We called this *exosystem* the "virtual" spacecraft. The advantage of this approach is that we could guarantee a priori that the trajectories of this exosystem are feasible and perfect tracking can be achieved. That is, given some reference trajectories $w(t)$ and $z(t)$ we could guarantee the existence of an angular velocity command $\omega(t)$ such that Eqs. (11) are satisfied. In general, it is not true that, given some arbitrary functions of time $w(t)$ and $z(t)$, there exists such a command $\omega(t)$. For example, given $w(t)$ for $t \geq 0$, one could solve Eq. (11)

for $\omega(t)$ from

$$\omega = \frac{2}{1-|w|^4}(\dot{w} - \dot{\bar{w}}w^2) \tag{48}$$

whenever $w \neq 1$. The last equation implies the constraint

$$\dot{z}(1-|w|^2) - 2\,\mathrm{Im}(\dot{w}\,\bar{w}) = 0 \tag{49}$$

which, in general, does not hold for arbitrary functions of time $w(t)$ and $z(t)$.

In this section we develop an approach to generate feasible trajectories for the system in Eq. (11). These trajectories, can then be used as reference trajectories for the tracking problem. In particular, given an initial point (w_0, z_0), a final point (w_f, z_f) and a time t_f, we seek time functions $w(t)$ and $z(t)$, defined over the interval $0 \le t \le t_f$, such that $(w(0), z(0)) = (w_0, z_0)$, $(w(t_f), z(t_f)) = (w_f, z_f)$ and Eq. (49) is satisfied for all $0 \le t \le t_f$. We call such trajectories *feasible* since they ensure the existence of a function $\omega(t)$ such that system in Eq. (11) is satisfied. Such an $\omega(t)$ can be found by Eq. (52) below. The functions $w(t)$ and $z(t)$ are then the solutions of system (11) with input $\omega(t)$, initial conditions (w_0, z_0) and final conditions (w_f, z_f).

To solve the feasible trajectory generation problem, we will use the notion of differential flatness (Fliess et al., 1992, 1995. A system is differentially flat if one can find a number of outputs (the same as the number of inputs) such that all states and inputs of the system can be written as algebraic functions of these flat outputs and their derivatives. Differentially flat systems are extremely nice since, they are equivalent[3] to an algebraic system, i.e., a system without dynamics. The downside of this approach is that most (nonlinear) systems are not flat. Also, to date, there does not exist a systematic way for finding the flat outputs,[4] although very often (if they exist) they have intrinsic physical significance. An additional problem may arise if the transformation from the flat output space to the state space is singular. In this paper we address all these problems for the underactuated spacecraft problem, and propose a simple parameterization of trajectories in the flat output space that satisfies all the constraints and avoids any singularities.

From now on, and for clarity of exposition, we switch from complex to real number notation. The kinematic model of an underactuated rigid body is then described by

$$\dot{w}_1 = \tfrac{1}{2}(1 + w_1^2 - w_2^2)\omega_1 + w_1 w_2 \omega_2, \tag{50a}$$

$$\dot{w}_2 = \tfrac{1}{2}(1 - w_1^2 + w_2^2)\omega_2 + w_1 w_2 \omega_1, \tag{50b}$$

$$\dot{z} = w_1\omega_2 - w_2\omega_1 \tag{50c}$$

or, compactly, by

$$\begin{bmatrix}\dot{w}_1\\ \dot{w}_2\\ \dot{z}\end{bmatrix} = \begin{bmatrix}\tfrac{1}{2}(1+w_1^2-w_2^2) & w_1w_2\\ w_1w_2 & \tfrac{1}{2}(1-w_1^2+w_2^2)\\ -w_2 & w_1\end{bmatrix}\begin{bmatrix}\omega_1\\ \omega_2\end{bmatrix} = F(w)\begin{bmatrix}\omega_1\\ \omega_2\end{bmatrix}. \tag{51}$$

If $[\dot{w}_1 \;\; \dot{w}_2 \;\; \dot{z}]^{\mathrm{T}}$ is in the range of $F(w)$, we can solve the previous equation uniquely for the angular velocities

$$\begin{bmatrix}\omega_1\\ \omega_2\end{bmatrix} = (F^{\mathrm{T}}(w)F(w))^{-1}F^{\mathrm{T}}(w)\begin{bmatrix}\dot{w}_1\\ \dot{w}_2\\ \dot{z}\end{bmatrix} = \frac{4}{(1+w_1^2+w_2^2)^2}\begin{bmatrix}\tfrac{1}{2}(1+w_1^2-w_2^2) & w_1w_2 & -w_2\\ w_1w_2 & \tfrac{1}{2}(1-w_1^2+w_2^2) & w_1\end{bmatrix}\begin{bmatrix}\dot{w}_1\\ \dot{w}_2\\ \dot{z}\end{bmatrix}. \tag{52}$$

Note that in case $[\dot{w}_1 \;\; \dot{w}_2 \;\; \dot{z}]^{\mathrm{T}}$ is not in the range of $F(w)$, the previous equation solves the minimum distance problem to the range of $F(w)$.

We now return to the characterization of the flat outputs of system (50).

Proposition 10. *The kinematic model of an underactuated rigid body described by Eqs.* (50) *is differentially flat.*

Consider the following two functions:

$$y_1 = 2\arctan\left(\frac{w_2}{w_1}\right) + z, \tag{53a}$$

$$y_2 = z. \tag{53b}$$

We claim that these are flat outputs for the system in Eqs. (50).

First note that, trivially, z can be written as a function of y_1 and y_2. Differentiating Eq. (53a) we get

$$\dot{y}_1 = \frac{1-|w|^2}{|w|^2}\dot{y}_2 + \dot{y}_2 = \frac{\dot{y}_2}{|w|^2} \tag{54}$$

or that

$$|w|^2 = \frac{\dot{y}_2}{\dot{y}_1}. \tag{55}$$

[3] This type of equivalence is called Lie–Bäcklund equivalence and it is quite well-known in physics. Two systems are equivalent in the Lie–Bäcklund sense if any variable of one system may expressed as a function of the variables of the other system and of a finite number of their time derivatives. One system can then be transformed to the other via endogenous feedback. This transformation does not necessarily preserve state dimension; see also Fliess, Levine, Martin and Rouchon (1999).

[4] Except the case of configuration flat Lagrangian systems with n degrees of freedom and $n-1$ controls, where a complete characterization exists; see, for instance, Murray and Rathinam (1996).

Moreover, we have that

$$\arctan\left(\frac{w_2}{w_1}\right) = \frac{y_1 - y_2}{2}. \tag{56}$$

The previous two equations together imply that

$$w_1 = \sqrt{\frac{\dot{y}_2}{\dot{y}_1}}\cos\left(\frac{y_1 - y_2}{2}\right), \tag{57a}$$

$$w_2 = \sqrt{\frac{\dot{y}_2}{\dot{y}_1}}\sin\left(\frac{y_1 - y_2}{2}\right) \tag{57b}$$

which, together with the equation,

$$z = y_2 \tag{58}$$

imply that w_1, w_2 and z can be written as algebraic functions of y_1, y_2 and their time derivatives. By virtue of Eq. (52) ω_1 and ω_2 can also be written as functions of y_1, y_2 and their time derivatives. Therefore, y_1 and y_2 are flat outputs for the system in Eqs. (50), as claimed.

The initial and final points of the trajectory correspond to the points

$$y_{10} = 2\arctan\left(\frac{w_{20}}{w_{10}}\right) + z_0, \quad y_{20} = z_0, \tag{59a}$$

$$y_{1f} = 2\arctan\left(\frac{w_{2f}}{w_{1f}}\right) + z_f, \quad y_{2f} = z_f \tag{59b}$$

in the y_1–y_2 plane, respectively. We can now construct paths in the y_1–y_2 plane connecting the points (y_{10}, y_{20}) and (y_{1f}, y_{2f}) and map them back to the w–z state space using Eqs. (53b). We may choose any path we want, as long as $\dot{y}_1\dot{y}_2 \geq 0$. One way to achieve this is to assume a linear dependence of y_1 with time

$$y_1(t) = y_{10} + \frac{t}{t_f}(y_{1f} - y_{10}) \tag{60}$$

and then parameterize y_2 as a cubic function of y_1

$$y_2 = a_0 + a_1 y_1 + a_2 y_1^2 + a_3 y_1^3. \tag{61}$$

Because the output y_2 is parameterized in terms of y_1, we call y_1 the "independent" flat output. The previous parameterization implies

$$y_2(0) = y_2(y_1(0)) = a_0 + a_1 y_1(0) + a_2 y_1^2(0) + a_3 y_1^3(0), \tag{62a}$$

$$y_2(t_f) = y_2(y_1(t_f)) = a_0 + a_1 y_1(t_f) + a_2 y_1^2(t_f) + a_3 y_1^3(t_f). \tag{62b}$$

From Eq. (55), the boundary conditions at $t = 0$ and t_f also imply the extra constraints

$$\frac{dy_2}{dy_1}(0) = a_1 + 2a_2 y_1(0) + 3a_3 y_1^2(0) = w_{10}^2 + w_{20}^2 = |w(0)|^2, \tag{63a}$$

$$\frac{dy_2}{dy_1}(t_f) = a_1 + 2a_2 y_1(t_f) + 3a_3 y_1^2(t_f) = w_{1f}^2 + w_{2f}^2 = |w(t_f)|^2. \tag{63b}$$

We have a linear system of four equations (62)–(63) in the four unknowns a_0, a_1, a_2, a_3. In order to ensure that $y_2'(y_1) \geq 0$ we take advantage of the ambiguity of the $\arctan(\cdot)$ function in Eqs. (53). First, and without loss of generality we assume that $y_{1f} > y_{10}$ and $y_{2f} \geq y_{20}$. Otherwise, we can add or subtract multiples of 4π to y_{i0} and/or y_{if} $(i = 1,2)$ to make sure that the previous inequalities hold.

From Eq. (61) we have that $y_2'(y_1) = 0$ whenever

$$y_1^* = \frac{-a_2 \pm \sqrt{a_2^2 - 3a_1 a_3}}{3a_3}. \tag{64}$$

By adding multiples of 4π to y_{2f} one can ensure that $y_1^* \notin (y_{10}, y_{1f})$. Since $y_2'(y_1)(0) \geq 0$ it follows that $y_2'(y_1)(t) \geq 0$ for all $t \in [0, t_f]$.[5]

Remark 11. One can choose many different paths connecting (y_{10}, y_{20}) and (y_{1f}, y_{2f}) in the y_1–y_2 plane, as long as they satisfy the boundary conditions in Eqs. (62) and (63). A cubic polynomial is the lowest degree polynomial which satisfies the four boundary conditions in Eqs. (62)–(63). Since the cubic polynomial is completely determined by these boundary conditions, there is no extra freedom to satisfy the slope constraint $y_2'(y_1) \geq 0$. One could have chosen a higher order polynomial and use the extra degrees of freedom to satisfy the slope constraint. However, this is not an easy task with no analytical answer. Here we have chosen the simplest case of a cubic polynomial, and we have addressed the slope restriction by taking advantage of the fact that multiples or 2π correspond to the same angle (i.e., the same physical orientation of the body).

Once the time functions $y_1(t)$ and $y_2(t)$ are known from the algorithm above, one can compute $\dot{w}_1$ and $\dot{w}_2$ and $\dot{z}$ from

$$\dot{w}_1 = \frac{1}{2}\left(\frac{\dot{y}_1}{\dot{y}_2}\right)^{1/2}\left(\frac{\ddot{y}_2}{\dot{y}_1} - \frac{\dot{y}_2\ddot{y}_1}{\dot{y}_1^2}\right)\cos\left(\frac{y_1 - y_2}{2}\right) - \left(\frac{\dot{y}_2}{\dot{y}_1}\right)^{1/2}\sin\left(\frac{y_1 - y_2}{2}\right)\frac{\dot{y}_1 - \dot{y}_2}{2}, \tag{65a}$$

[5] A proof of this result is shown in the appendix.

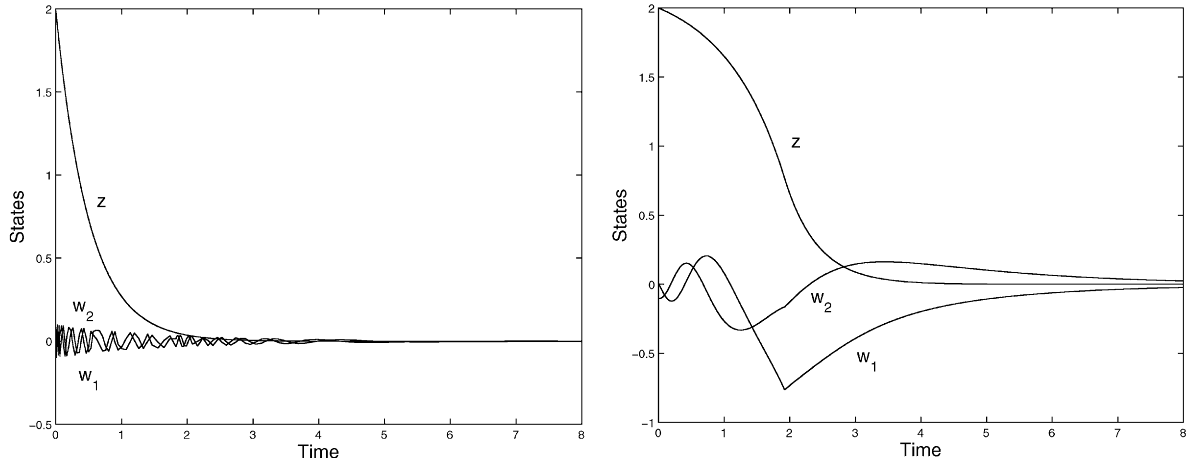

(a) Closed-loop trajectories with control in Eq. (12). (b) Closed-loop trajectories with control in Eq. (15).

Fig. 4. Closed-loop trajectories for the system of equation (11).

$$\dot{w}_2 = \frac{1}{2}\left(\frac{\dot{y}_1}{\dot{y}_2}\right)^{1/2}\left(\frac{\ddot{y}_2}{\dot{y}_1} - \frac{\dot{y}_2\ddot{y}_1}{\dot{y}_1^2}\right)\sin\left(\frac{y_1 - y_2}{2}\right) - \left(\frac{\dot{y}_2}{\dot{y}_1}\right)^{1/2}\cos\left(\frac{y_1 - y_2}{2}\right)\frac{\dot{y}_1 - \dot{y}_2}{2}, \tag{65b}$$

$$\dot{z} = \dot{y}_2, \tag{65c}$$

where $\dot{y}_1 \neq 0$ because of Eq. (60). The corresponding angular velocities are computed from Eq. (52).

Eqs. (65) have a potential singularity at $\dot{y}_2 = 0$. By the previous discussion it is clear that this can happen only at the boundary points of the interval $[0, t_f]$. Indeed, if either $|w(0)| = 0$ or $|w(t_f)| = 0$, then from Eq. (55) we must have necessarily $\dot{y}_2(0) = 0$ or $\dot{y}_2(t_f) = 0$, respectively. From Eqs. (65) it is clear that in such a case we need to impose the additional constraint that $\ddot{y}_2(0) = 0$ or $\ddot{y}_2(t_f) = 0$.

Since

$$\ddot{y}_2(t) = (2a_2 + 6a_3 y_1(t))\dot{y}_1^2(t), \tag{66}$$

we can guarantee that $\ddot{y}_2(0) = 0$ by choosing a function $y_1(t)$ such that $\dot{y}_1(0) = 0$. For instance, if $|w(0)| = 0$ we can choose

$$y_1(t) = y_{10} + \left(\frac{t}{t_f}\right)^2 (y_{1f} - y_{10}). \tag{67}$$

Similarly, for the case when $|w(t_f)| = 0$ we can choose the following time parameterization for y_1:

$$y_1(t) = y_{1f} + \left(\frac{t - t_f}{t_f}\right)^2 (y_{10} - y_{1f}) \tag{68}$$

which guarantees that $\dot{y}_1(t_f) = 0$ and hence from Eq. (66) also that $\ddot{y}_2(t_f) = 0$.

Finally, for the case when the initial and final conditions are such that $|w(0)| = |w(t_f)| = 0$, we can choose the following cubic parameterization of y_1:

$$y_1(t) = 2(y_{10} - y_{1f})\left(\frac{t}{t_f}\right)^3 - 3(y_{10} - y_{1f})\left(\frac{t}{t_f}\right)^2 + y_{10}. \tag{69}$$

This expression guarantees that $\dot{y}_1(0) = \dot{y}_1(t_f) = 0$, hence also that $\ddot{y}_2(0) = \ddot{y}_2(t_f) = 0$, as required. Notice that the parameterizations of $y_1(t)$ given in Eqs. (67)–(69) ensure that $\dot{y}_1(t) \neq 0$ for all $t \in (0, t_f)$.

Summarizing, we have shown that a linear parameterization for "independent" flat output $y_1(t)$ along with a cubic parameterization of y_2 in terms of y_1 can be used to solve the trajectory generation problem in the flat output space for the majority of cases. With a linear parameterization of y_1, singularities may occur at the initial and/or final points, if $|w| = 0$ at these points. If this is the case, a quadratic or cubic parameterization of y_1 can be used to circumvent the singularity problem at the boundary points.

7. Numerical examples

In this section we provide numerical examples to demonstrate the control laws developed previously. The first example compares the control laws in Eqs. (12) and (15). The initial conditions were chosen as $w(0) = 0.01 - i0.1$ and $z(0) = 2$. These initial conditions were chosen on purpose close to the singular manifold $w = 0$ in order to demonstrate the effect of "bad" initial conditions. The time histories of the corresponding closed-loop trajectories are shown in Fig. 4. For the control law in Eq. (15) the gains were chosen as $\kappa = 1$ in $\mathscr{D}_g$ and $\kappa = -2$ in $\mathscr{D}_b$, and $\mu = 2$. For the control law in Eq. (12) it is $\kappa = 1$.

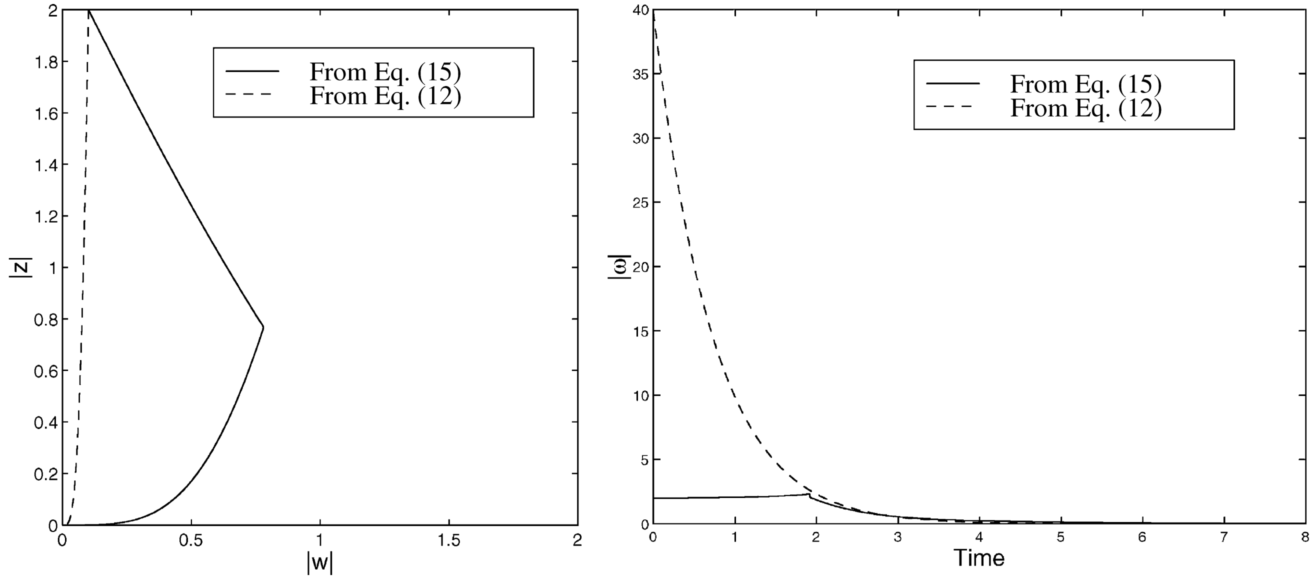

(a) Comparison of closed-loop trajectories. (b) Comparison of control inputs.

Fig. 5. Comparison of closed-loop trajectories and control inputs with control laws as in Eqs. (12) and (15).

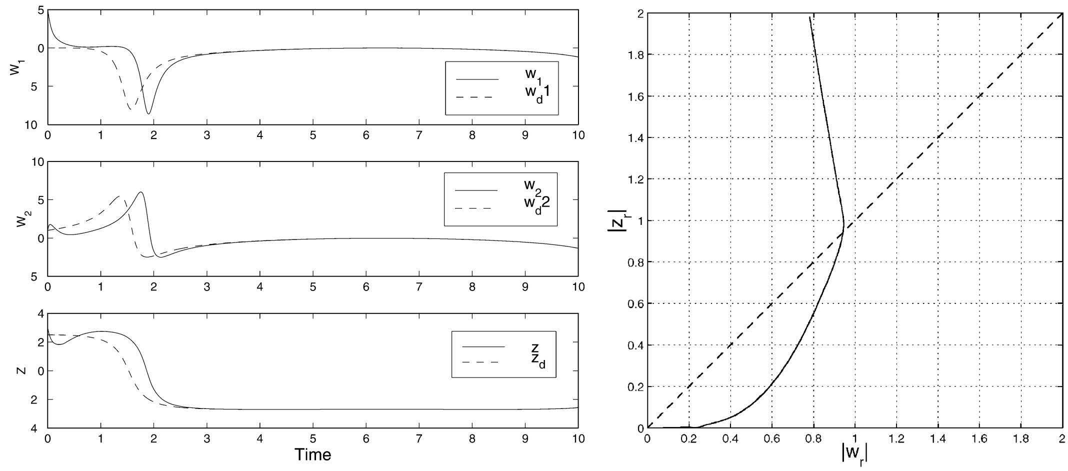

(a) Time histories of the actual and reference trajectories. (b) Trajectories of error system in $(|w_r|, |z_r|)$ space.

Fig. 6. Closed-loop trajectories for the tracking problem.

The corresponding trajectories in the (w, z) plane are shown in Fig. 5(a). The solid line corresponds to the trajectory using the bounded control law in Eq. (15), while the dashed line corresponds to the trajectory using the control law in Eq. (12). Fig. 5(b) shows the dramatic reduction in the control input required to perform this maneuver using the control in Eq. (15). In this case, the control law is bounded by $\max\{|\kappa|\} + \mu = 4$ as suggested by Proposition 3. The control reduction is achieved by allowing the states w_1 and w_2 increase at the beginning of the trajectory so as to move away from the singular manifold $w = 0$; see also Fig. 4.

The second example deals with the attitude tracking problem. We again consider the kinematic equations of a rigid body, described by Eqs. (11). We let the trajectory to be tracked generated by the system in Eqs. (25) where $\omega_d(t) = 0.5\sin(0.5t) + \mathrm{i}\cos(0.25t)$. The initial conditions are given by $(w(0), z(0)) = (5 + \mathrm{i}, 3)$ and $(w_d(0), z_d(0)) = (\mathrm{i}, 2.5)$. The results of the numerical simulations are shown in Fig. 6. The closed-loop trajectories with control law as in Eq. (35) are shown in Fig. 6(a). The gains were chosen as $\kappa = 2$ in $\mathscr{D}_{\mathrm{g}}$ and $\kappa = -1$ in $\mathscr{D}_{\mathrm{b}}$, and $\mu = 4$. Fig. 6(b) shows the error trajectories in the $(|w_r|, |z_r|)$ space.

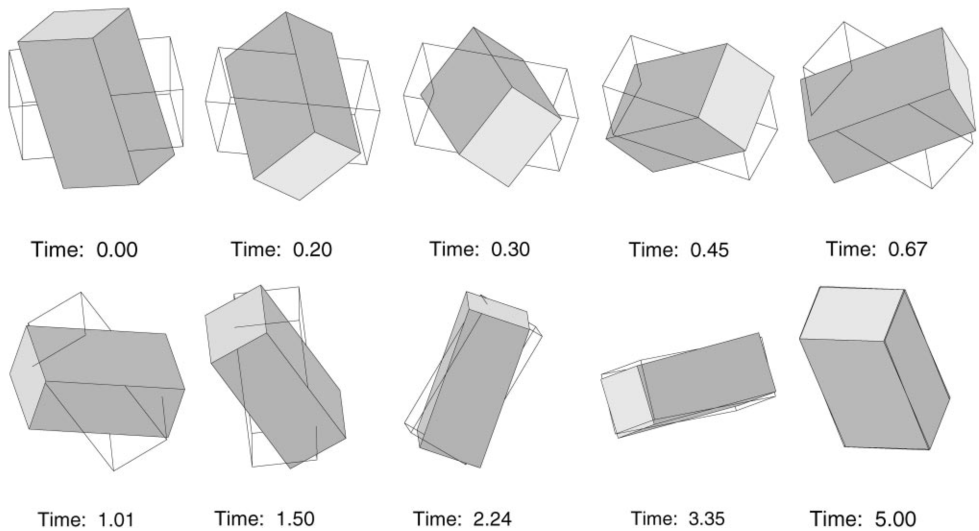

Fig. 7. Snapshots of the attitude orientation history. The wire frame represents the "virtual" spacecraft which furnishes the reference attitude to be tracked.

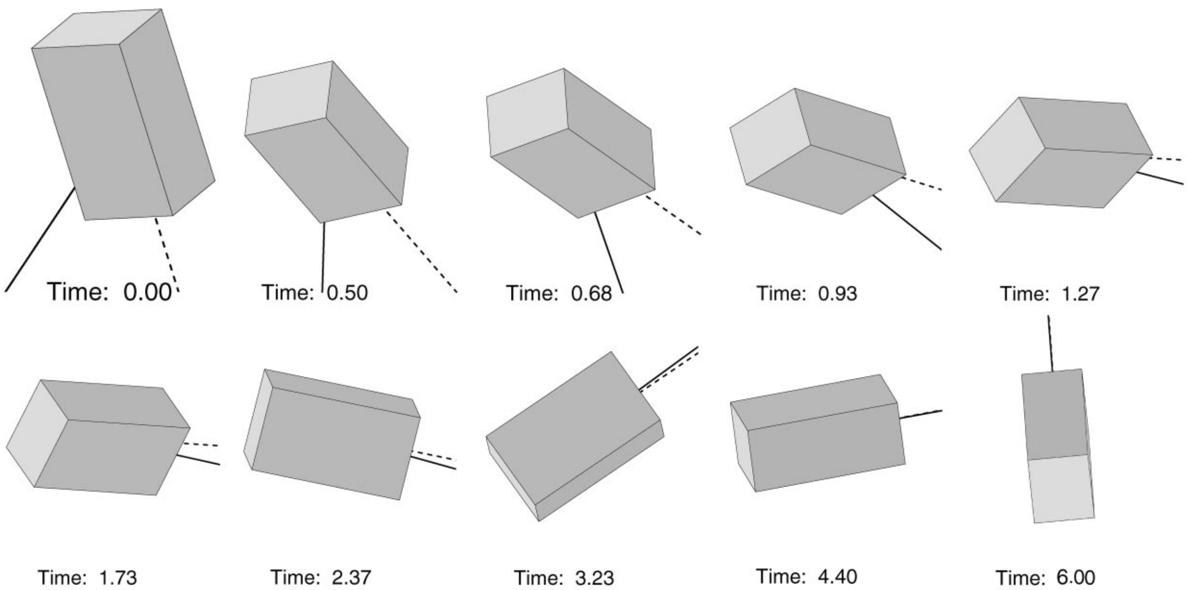

Fig. 8. Snapshots of the attitude orientation history for the reference direction tracking problem. The solid line represents the desired direction in inertial frame and the dashed line represents the symmetry axis.

Fig. 7 shows a series of "snapshots" of the actual orientation of the body and the target reference frames. The solid parallelepiped in the figure represents the rigid spacecraft while the wire frame represents the "virtual" spacecraft along the desired attitude history. Fig. 7 shows clearly that tracking of the target frame has been achieved after approximately 5 s in this case.

The next example demonstrates tracking of a desired *direction* in inertial space. The body is assumed axisymmetric having a constant velocity component about the $\hat{b}_3$-axis equal to $\omega_{30} = -0.5$ r/s. The control law in Eq. (41) is used with $\kappa = 2$. The reference trajectory for the unit vector $\hat{v}_3$ is generated by the system in Eqs. (25a) with $\omega_d(t) = t\sin(0.5t) + \mathrm{i}1.5\cos(t)$.

The actual orientation of the spacecraft during the tracking maneuver is shown in Fig. 8. The solid line in Fig. 8 represents the desired reference direction $\hat{v}_3$ and the dashed line represent the body axis direction $\hat{b}_3$. Fig. 8 shows that tracking of $\hat{v}_3$ has been achieved after approximately 4 s.

In the last example, we demonstrate the algorithm for automatic feasible trajectory generation developed in Section 6. We assume first that the initial and final conditions are given by $(w_1(0), w_2(0), z(0)) = (1, 2, 0.5)$ and

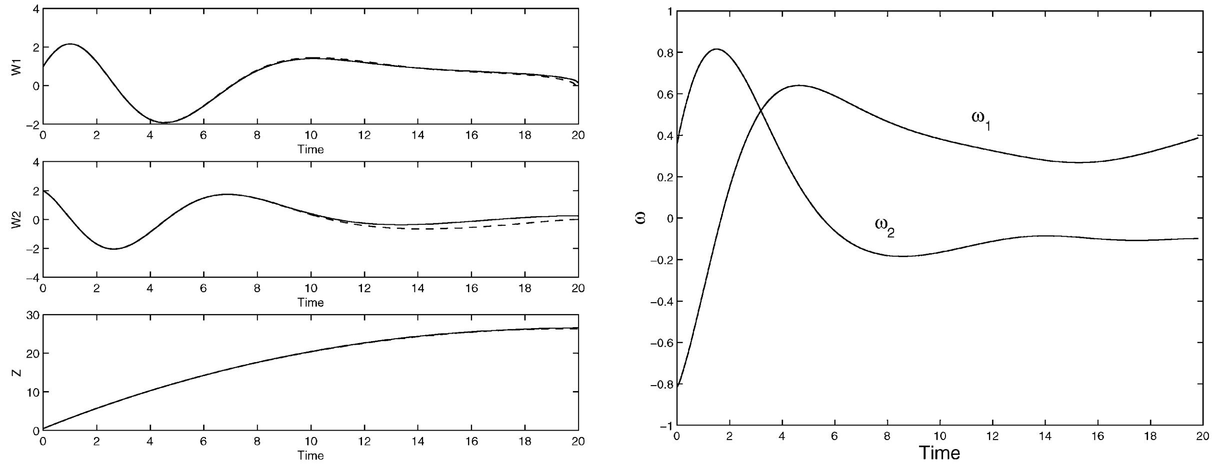

(a) Trajectories in $w-z$ space.

(b) Angular velocity commands.

Fig. 9. Feasible trajectory generation.

$(w_1(t_f), w_2(t_f), z(t_f)) = (0, -1, 1.25)$, respectively. We also choose $t_f = 20$ s. The corresponding initial and final points in the y_1–y_2-plane of the flat outputs are calculated by the proposed algorithm as $(y_{10}, y_{20}) = (2.71, 0.5)$ and $(y_{1f}, y_{2f}) = (10.67, 13.81)$. Notice that in this case $y_{1f} = 2\,\mathrm{atan}[w_2(t_f)/w_1(t_f)] + z(t_f) + 4\pi$ and $y_2(t_f) = 4\pi + z(t_f)$. Fig. 9(a) shows the trajectories in the w–z space, and Fig. 9(b) shows the corresponding angular velocity history which generates these trajectories. In Fig. 9(a) there are actually plotted two separate sets of trajectories. One set is generated from the flat outputs, i.e., from Eqs. (58), and the other set is generated directly from the dynamical equations (11) subject to the angular velocity history in Fig. 9(b). The two sets are almost exact so there is no visible discrepancy in Fig. 9(a). Fig. 10 shows the corresponding path in the flat output space.

Consider now the case when $(w_1(t_f), w_2(t_f), z(t_f)) = (0, 0, 1.25)$. The initial conditions remain the same as in the previous case. If we use the linear parameterization for y_1 given in Eq. (60) we get the results in Fig. 11. The dashed lines in Fig. 11(a) correspond to the trajectories as given directly by the flat outputs, and the solid lines correspond to the trajectories as given by integrating the system of differential equations using the angular velocity history in Fig. 11(b). Notice that although the trajectory generated by the flat output approach matches very closely the one generated by the dynamical system, the angular velocity history requires large values at the final point. In particular, because of the singularity at that point, we get that $\lim_{t\to t_f} \dot{\omega}(t) = \infty$.

By using the quadratic parameterization of $y_1(t)$ in Eq. (68) we get the results in Fig. 12. The trajectories are shown in Fig. 12(a). They are similar to the previous ones (since the path in the flat output space remains the same). The angular velocity history, however, shown in Fig. 12(b) is much better behaved. In particular, the singularity at the final time has been eliminated completely.

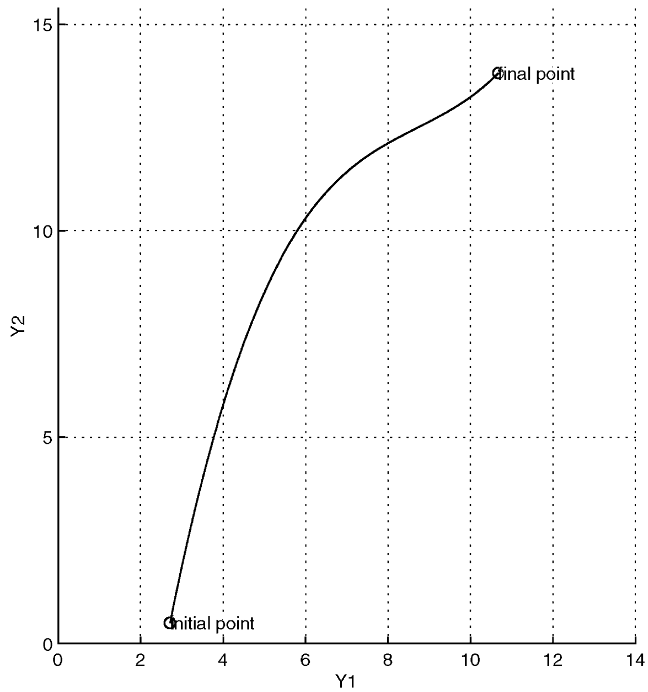

Fig. 10. Corresponding trajectories in the flat output space.

Similar results are obtained for boundary conditions such that $|w(0)| = 0$ and $|w(0)| = |w(t_f)| = 0$. In the latter case, the cubic parameterization of $y_1(t)$ in Eq. (69) can be used to obtain well-behaved angular velocity command at both the initial and the final time.

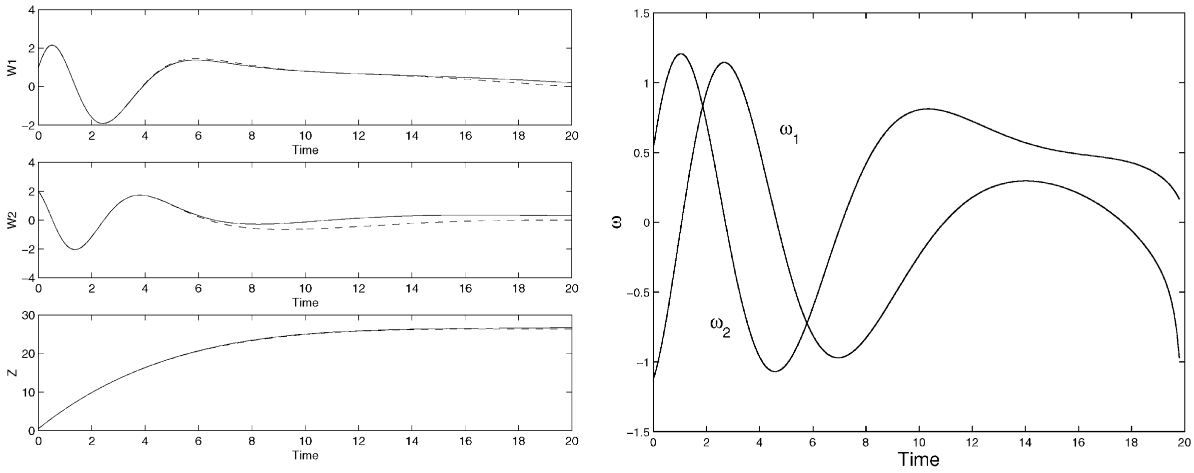

(a) Trajectories in $w-z$ space. (b) Angular velocity commands.

Fig. 11. Feasible trajectory generation using a linear parameterization for y_1 (case $|w(t_f)| = 0$).

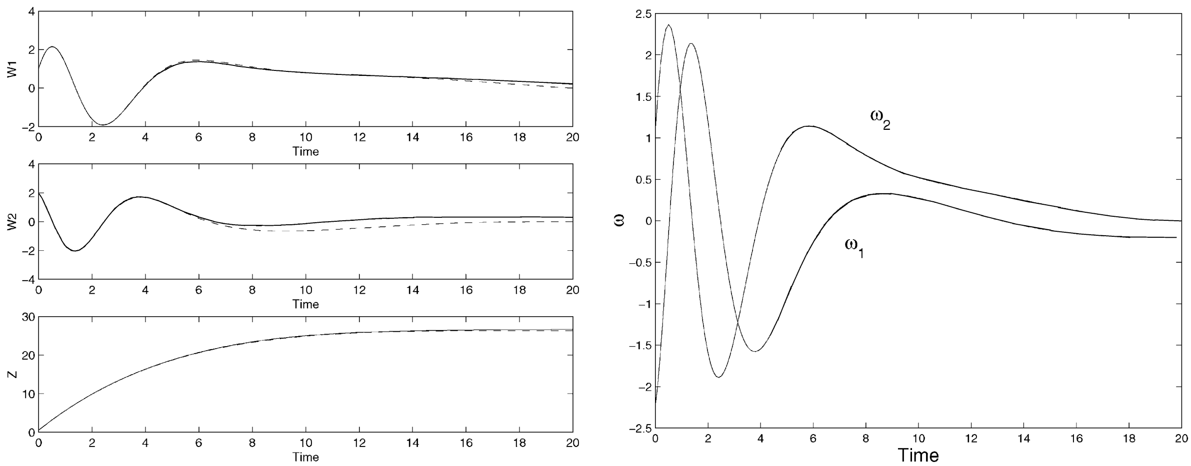

(a) Trajectories in $w-z$ space. (b) Angular velocity commands.

Fig. 12. Feasible trajectory generation using a quadratic parameterization for y_1 (case $|w(t_f)| = 0$).

8. Conclusions

In this paper we solve the problems of stabilization and tracking for an underactuated rigid spacecraft. The body is underactuated in the sense that there is no control authority along one of its principal axis. An example of this situation is the case of an axisymmetric rigid spacecraft with a thruster failure along the symmetry axis. For the restricted case of zero spin rate, stabilization is possible, but any stabilizing control laws has to be nonsmooth. We develop such a nonsmooth control law which, in addition, remains bounded by an a priori specified bound. We then extend these stabilization results to controllers which are able to track a given attitude trajectory. As a special case, we also present a control law to track an arbitrary direction in the inertial space using two bounded control inputs. All proposed control laws achieve asymptotically stability and tracking with (asymptotic) exponential convergence rates for all initial conditions. In addition to the previous results, we give an algorithm for feasible trajectory generation for an underactuated axi-symmetric rigid body. These feasible trajectories can then be used as reference trajectories for the tracking problem. The proposed algorithm is especially simple and is based on the differential flatness of the corresponding differential equations. The whole approach can be readily automated and can thus be used for autonomous, on-line trajectory generation and tracking without user intervention. One of the novelties of the proposed approach is the use of a recently developed, nonstandard coordinate attitude parameterization which can be used to isolate the motion of the underactuated axis from the general motion of the body.

Acknowledgements

This work has been supported by the National Science Foundation under Grant CMS-96-24188.

Appendix

Consider the curve in the y_1–y_2 plane given by

$$y_2 = a_0 + a_1 y_1 + a_2 y_1^2 + a_3 y_1^2, \tag{A.1}$$

where a_0, a_1, a_2, a_3 are given by the solution to the following linear set of equations:

$$\begin{bmatrix} 1 & y_{10} & y_{10}^2 & y_{10}^3 \\ 1 & y_{1f} & y_{1f}^2 & y_{1f}^3 \\ 0 & 1 & 2y_{10} & 3y_{10}^2 \\ 0 & 1 & 2y_{1f} & 3y_{1f}^2 \end{bmatrix} \begin{bmatrix} a_0 \\ a_1 \\ a_2 \\ a_3 \end{bmatrix} = \begin{bmatrix} y_{20} \\ y_{2f} \\ w_0^2 \\ w_f^2 \end{bmatrix} \tag{A.2}$$

and where $y_{10}, y_{1f}, y_{20}, w_0^2$ and w_f^2 are positive constants, with $y_{1f} > y_{10}$.

We will show that, under these conditions, there always exist a y_{2f} large enough (positive), such that

$$\frac{dy_2}{dy_1} \geq 0. \tag{A.3}$$

To this end, calculation of the previous derivative gives

$$y_2' = a_1 + 2a_2 y_1 + 3a_3 y_1^2. \tag{A.4}$$

Clearly,

$$\min y_2' = y_2(y_1^*) = a_1 - \frac{a_2^2}{3a_3}, \tag{A.5}$$

where y_1^* as in Eq. (64). Since by assumption, $y_2'(y_{10}) > 0$ and $y_2'(y_{1f}) > 0$, then Eq. (A.3) holds if and only if $a_1 - a_2/3a_3 \geq 0$.

A tedious but straightforward calculation shows that a_1, a_2 and a_3 are linear functions of y_{2f} given by

$$a_1 = -6\frac{y_{10} y_{1f}}{(y_{1f} - y_{10})^3} y_{2f} + c_1, \tag{A.6a}$$

$$a_2 = 3\frac{y_{10} + y_{1f}}{(y_{1f} - y_{10})^3} y_{2f} + c_2, \tag{A.6b}$$

$$a_3 = -2\frac{1}{(y_{1f} - y_{10})^3} y_{2f} + c_3, \tag{A.6c}$$

where c_1, c_2 and c_3 are constants independent of y_{2f}.

Substituting Eqs. (A.6) in the r.h.s. of Eq. (A.5) and for large enough y_{2f}, one obtains that

$$a_1 - \frac{a_2^2}{3a_3} \approx \frac{3}{2(y_{1f} - y_{10})} y_{2f} + c, \tag{A.7}$$

where c is a constant independent of y_{2f}.

Since by assumption $y_{1f} - y_{10} > 0$, the last equation shows that for y_{2f} large enough we have that $y_2'(y_1) \geq 0$ and the proof is complete.

References

Aeyels, D., & Szafranski, M. (1988). Comments on the stabilizability of the angular velocity of a rigid body. *Systems and Control Letters*, *10*(1), 35–39.

Andriano, V. (1993). Global feedback stabilization of the angular velocity of a symmetric rigid body. *Systems and Control Letters*, *20*, 361–364.

Bach, R., & Paielli, R. (1993). Linearization of attitude-control error dynamics. *IEEE Transactions on Automatic Control*, *38*(10), 1521–1525.

Byrnes, C. I., & Isidori, A. (1991). On the attitude stabilization of a rigid spacecraft. *Automatica*, *27*(1), 87–95.

Coron, J. M., & Kerai, E. L. (1996). Explicit feedback stabilizing the attitude of a rigid spacecraft with two control torques. *Automatica*, *36*(5), 669–677.

Crouch, P. E. (1984). Spacecraft attitude control and stabilization: Applications of geometric control theory to rigid body models. *IEEE Transactions on Automatic Control*, *29*(4), 321–331.

Darboux, G. (1887). *Leçons sur la Théorie Générale des Surfaces*, Vol. 1. Paris: Gauthier-Villars.

Fliess, M., Levine, J., & Rouchon, P. (1992). On differentially flat nonlinear systems. *Comptes Rendus des S'eqnces de l' Acad'emie des Sciences*, *315*, 619–624.

Fliess, M., Levine, J., Martin, Ph., & Rouchon, P. (1995). Flatness and defect of nonlinear systems: Introductory theory and examples. *International Journal of Control*, *61*(9), 1327–1361.

Fliess, M., Levine, J., Martin, P., & Rouchon, P. (1999). A Lie–Bäcklund approach to equivalence and flatness of nonlinear systems. *IEEE Transactions on Automatic Control*, *44*(5), 922–937.

Khennouf, H., & Canudas de Wit, C. (1995). On the construction of stabilizing discontinuous controllers for nonholonomic systems. In *Proceedings of IFAC nonlinear control system design symposium*, Tahoe City, CA (pp. 747–752).

Krishnan, H., McClamroch, H., & Reyhanoglu, M. (1992). On the attitude stabilization of a rigid spacecraft using two control torques. In *Proceedings of the American control conference*, Chicago, IL (pp. 1990–1995).

Luo, J., & Tsiotras, P. (1998). Control design for systems in chained form with bounded inputs. In *Proceedings of the American control conference*, Philadelphia, PA (pp. 473–477).

Morin, P., & Samson, C. (1997). Time-varying stabilization of a rigid spacecraft with two control torques. *IEEE Transactions on Automatic Control*, *42*(4), 528–534.

Morin, P., Samson, C., Pomet, J. B., & Jiang, Z. -P. (1995). Time-varying feedback stabilization of the attitude of a rigid spacecraft with two controls. *Systems and Control Letters*, *25*, 375–385.

Murray, R. M., & Rathinam, M. (1996). Configuration flatness of Lagrangian systems underactuated by one control. In *Proceedings, 35th conference on decision and control*, Kobe, Japan (pp. 1688–1693).

Nieuwstadt, M. J., & Murray, R. M. (1995). Approximate trajectory generation for differentially flat systems with zero dynamics. In *Proceedings of 34th IEEE conference on decision and control*, New Orleans, LA (pp. 4224–4230).

Outbib, R., & Sallet, G. (1992). Stabilizability of the angular velocity of a rigid body revisited. *Systems and Control Letters*, *18*(2), 93–98.

Schleicher, A. (1999). *Partial attitude stabilization of a rigid body spacecraft using two control torques*. Master's thesis, Georgia Institute of Technology, Atlanta, GA.

Shuster, M. D. (1993). A survey of attitude representations. *Journal of the Astronautical Sciences*, *41*(4), 439–517.

Sontag, E., & Sussmann, H. (1988). Further comments on the stabilizability of the angular veloctiy of a rigid body. *Systems and Control Letters*, *12*(3), 213–217.

Sørdalen, O. J., Egeland, O., & Canudas de Wit, C. (1992). Attitude stabilization with a nonholonomic constraint. In *Proceedings of the 31st conference on decision and control*, Tuscon, AZ (pp. 1610–1611).

Tsiotras, P., & Luo, J. (1997). Reduced-effort control laws for underactuated rigid spacecraft. *Journal of Guidance, Control, and Dynamics*, *20*(6), 1089–1095.

Tsiotras, P., & Longuski, J. M. (1994). Spin-axis stabilization of symmetric spacecraft with two control torques. *Systems and Control Letters*, *23*(6), 395–402.

Tsiotras, P., & Longuski, J. M. (1995). A new parameterization of the attitude kinematics. *Journal of the Astronautical Sciences*, *43*(3), 243–262.

Tsiotras, P., & Longuski, J. M. (1996). Comments on a new parameterization of the attitude kinematics. In *AIAA/AAS astrodynamics specialists conference*, San Diego, CA. Paper AAS 96-3627.

Tsiotras, P., Corless, M., & Longuski, M. (1995). A novel approach for the attitude control of an axisymmetric spacecraft subject to two control torques. *Automatica*, *31*(8), 1099–1112.

Wen, J. T., & Kreutz-Delgado, K. (1991). The attitude control problem. *IEEE Transactions on Automatic Control*, *36*(10), 1148–1162.

Dr. Tsiotras joined the faculty of the School of Aerospace Engineering at the Georgia Institute of Technology in 1998. Prior to joining the faculty at Georgia Tech, Dr. Tsiotras was an Assistant Professor of Mechanical and Aerospace Engineering at the University of Virginia. From 1993 to 1994 he was a Post-doctoral Fellow at Purdue University, and during 1989 he was affiliated with the Interdisciplinary Center of Applied Mathematics at the Virginia Polytechnic Institute and State University. Dr. Tsiotras holds a Ph.D. degree in Aeronautics and Astronautics (Purdue University, 1993), an M.Sc. degree in Mathematics (Purdue University, 1992), an M.Sc. in Aerospace Engineering (VPI&SU, 1987) and a Dilp.Eng. in Mechanical Engineering (National Technical University of Athens, Greece, 1986). His current research interests include analysis and control of nonlinear dynamical systems emphasizing kinematics and dynamics of rotating systems, robust and optimal control of mechanical and aerospace systems, and control of underactuated systems. Dr. Tsiotras is a recipient of the NSF CAREER Award, the Sigma Xi President and Visitor's Award for Excellence in Research from the University of Virginia, as well as numerous fellowships and scholarships. He is an Associate Editor for the Journal of Guidance, Control, and Dynamics and for Dynamics and Control. He is a senior member of the AIAA, and a member of the ASME, IEEE and ASEE, as well as a member of the Phi Kappa Phi, Tau Beta Pi and Sigma Gamma Tau honor societies.

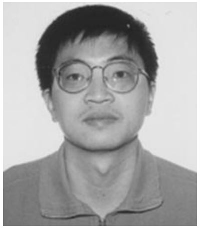

Jihao Luo was born in Shaoxing, Zhejiang, China in 1968. He received his BS degree in Mechanical Engineering at Zhejiang University, in July 1990, and his M.Sc. in Mechanical Engineering at Zhejiang University, in March 1993. From April 1993 to July 1995, he was working at the Institute for Fluid Power Transmission and Control at Zhejiang University. He received his Ph.D. in Mechanical Engineering at the University of Virginia, in December 1999. He was twice in the final list for the Best Student Paper Award of the American Control Conferences in 1997 and 1998. His main interests are in nonlinear control design for mechanical systems, and robust control implementation.